J. Fluid Mech. (1977), *vol.* 82, *part* 1, *pp.* 17–28
Printed in Great Britain

Nonlinear wave propagation in a two-dimensional steady transonic flow

By PHOOLAN PRASAD AND E. V. KRISHNAN

Mehta Research Institute of Mathematics and Mathematical Physics,
26 Dilkusha, New Katra, Allahabad-211002 (U.P.), India†

(Received 15 November 1976)

When we look at photographs of real transonic flows which are predicted to be shockless, we find a very large number of weak shocks almost perpendicular to the streamlines. These are no more than almost-trapped upstream-propagating nonlinear waves. In this paper we try to obtain a simple approximate equation which gives their complete history and takes into account both their turning effect, owing to a non-zero gradient of the fluid velocity in a direction normal to the streamlines, and also the finite radius of curvature of the wave front. We first give a brief discussion of a few results which can be easily obtained from the solution of the approximate equation and then compute the history of two nonlinear pulses by numerically integrating the equation.

1. Introduction

Recently some interest has been revived in the propagation of weak pulses in a transonic flow (Prasad 1973) in order to resolve the famous transonic controversy. It was initially proposed that, owing to trapping of upstream-propagating waves at different points of a sonic surface, a continuous mixed supersonic and subsonic flow is unstable (Kuo 1951). Using methods of geometrical acoustics, Spee (1971) calculated the motion of the wave front and showed that, owing to the variation of the flow variables in the directions normal to the streamlines, a wave front perpendicular to the streamlines turns and thus escapes being trapped in the transonic region. Still, when we look at photographs of a transonic flow (Spee 1971) we observe the presence of a large number of weak shocks perpendicular to the streamlines and moving slowly in the transonic region.

The upstream-propagating waves perpendicular to the streamlines, for which each of the bicharacteristic velocity components vanishes at a sonic point, remain in the transonic region for a longer time compared with other waves and this explains the existence of almost-trapped waves with weak shocks in a transonic flow. Prasad (1973) discussed the propagation of these trapped waves by assuming the wave front to be plane and perpendicular to the streamlines. Owing to this assumption he could not take into account the important multi-dimensional turning effect. Under the assumption that a characteristic length in the steady state and the radius of curvature of the wave front are large compared with the extent of the wave in the direction

† Present address: Department of Applied Mathematics, Indian Institute of Science, Bangalore-560012, India.

normal to the wave front, and that the angle between the normal to the wave front and the streamlines is small, we can easily discuss the turning effect of the waves by using a model equation which has been derived by Prasad (1975). This model equation, governing the motion of the perturbations to the steady flow, is a quasi-linear partial differential equation which completely takes into account the curvature of the wave front, the nonlinear steepening of the pulse and the two-dimensional turning effect and gives the complete history of the pulse as it moves in the transonic region.

We present here a local analysis of the model equation in the neighbourhood of points on the sonic line, assuming the initial wave front to be plane. In the neighbourhood of sonic points we use the local analysis to discuss the motion of the pulse in two special cases: (i) when the initial value of the angle θ between the normal to the wave front and the x_1 direction is zero and (ii) when the initial value of θ is non-zero.

2. Derivation of the approximate equation using thin-aerofoil theory

In order to avoid duplication and save space, we shall simply refer to the work of Prasad (1975) without defining the various symbols. In Prasad's paper there are two parameters: (i) ϵ, which is a measure of the extent of the wave in the normal direction, and (ii) δ, which is of the same order as the amplitude of the perturbations. Here we take δ and ϵ both to be small and of the same order in magnitude.

From the unsteady equations of motion of an inviscid non-conducting polytropic gas, the approximate equation for the perturbations is (see § 3 of Prasad 1975)

$$\frac{\partial \omega}{\partial t} + (q_\alpha - a n_\alpha)\frac{\partial \omega}{\partial x_\alpha} = (K - a_0\,\Omega)\,\omega, \tag{2.1}$$

where
$$K = -\frac{\gamma}{2}\frac{\partial q_{\alpha 0}}{\partial x_\alpha} - \tfrac{1}{2} n_\alpha n_\beta \frac{\partial q_{\beta 0}}{\partial x_\alpha} - \tfrac{1}{2}(q_{\alpha 0} - a_0 n_\alpha)\frac{1}{\rho_0 a_0}\frac{\partial}{\partial x_\alpha}(\rho_0 a_0) \tag{2.2}$$

and
$$\Omega = -\tfrac{1}{2}\,\partial n_\alpha / \partial x'_\alpha. \tag{2.3}$$

Here $\partial/\partial x'_\alpha$ is an interior derivative in the characteristic surface and is given by

$$\frac{\partial}{\partial x'_\alpha} = \frac{\partial}{\partial x_\alpha} + \frac{n_\alpha}{c_L}\frac{\partial}{\partial t}, \quad c_L = a - n_\alpha q_\alpha. \tag{2.3a}$$

If the wave is not headed by a shock, the flow variables are continuous across the wave front, which can be determined by solving the following equations along rays:

$$dx_1/dt = q_{10} - a_0 \cos\theta, \tag{2.4}$$

$$dx_2/dt = q_{20} - a_0 \sin\theta \tag{2.5}$$

and

$$\frac{d\theta}{dt} = \cos\theta \sin\theta \frac{\partial q_{10}}{\partial x_1} + \sin^2\theta \frac{\partial q_{20}}{\partial x_1} - \cos^2\theta \frac{\partial q_{10}}{\partial x_2} - \sin\theta\cos\theta \frac{\partial q_{20}}{\partial x_2} - \sin\theta \frac{\partial a_0}{\partial x_1} + \cos\theta \frac{\partial a_0}{\partial x_2}, \tag{2.6}$$

where θ is the angle which the unit normal to the wave front makes with the x_1 axis.

Now we use the assumptions of thin-aerofoil theory and therefore introduce the following non-dimensional variables:

$$q_{10} = a^* + \tau a^* \bar{q}_{10}, \quad q_{20} = \tau^{\frac{3}{2}} a^* \bar{q}_{20}, \tag{2.7), (2.8}$$

$$\bar{x}_1 = x_1/l, \quad \bar{x}_2 = \tau^{\frac{1}{2}} x_2/l, \tag{2.9}$$

where τ is a small parameter, l the length of the aerofoil (Guderley 1962) and a star indicates the values of the quantity at a sonic point (x_1^*, x_2^*). From Bernoulli's equation, we get the following expression for the sound speed:

$$a_0 = a^*[1 - \tfrac{1}{2}(\gamma-1)\,\tau \bar{q}_{10} - \tfrac{1}{8}(\gamma-1)(\gamma+1)\,\tau^2 \bar{q}_{10}^2] + O(\tau^3). \tag{2.10}$$

From (2.6) and (2.10) we get

$$\begin{aligned}\frac{1}{a^*}\frac{d\theta}{dt} = &-\tau^{\frac{3}{2}}\frac{\partial \bar{q}_{10}}{\partial \bar{x}_2} - \frac{\gamma-1}{2}\tau^{\frac{3}{2}}\frac{\partial \bar{q}_{10}}{\partial \bar{x}_2} - \tfrac{1}{8}(\gamma-1)(\gamma+1)\tau^{\frac{5}{2}}\frac{\partial(\bar{q}_{10}^2)}{\partial \bar{x}_2} \\ &+ \theta\left[\tau\frac{\partial \bar{q}_{10}}{\partial \bar{x}_1} - \tau^2\frac{\partial \bar{q}_{20}}{\partial \bar{x}_2} + \frac{\gamma-1}{2}\tau\frac{\partial \bar{q}_{10}}{\partial \bar{x}_1} + \tfrac{1}{8}(\gamma-1)(\gamma+1)\tau^2\frac{\partial(\bar{q}_{10}^2)}{\partial \bar{x}_1}\right] \\ &+ \theta^2\left[\tau^{\frac{3}{2}}\frac{\partial \bar{q}_{20}}{\partial \bar{x}_1} - \tau^{\frac{3}{2}}\frac{\partial \bar{q}_{10}}{\partial \bar{x}_2} + \tfrac{1}{4}(\gamma-1)\tau^{\frac{3}{2}}\frac{\partial \bar{q}_{10}}{\partial \bar{x}_2} + \tfrac{1}{16}(\gamma-1)(\gamma+1)\tau^{\frac{5}{2}}\frac{\partial(\bar{q}_{10}^2)}{\partial \bar{x}_2}\right] \\ &+ O(\tau^3) + O(\theta^3).\end{aligned} \tag{2.11}$$

Case 1. When $1 \gg |\theta| \gg \tau^{\frac{1}{2}}$, the dominant terms give

$$\frac{1}{a^*}\frac{d\theta}{dt} = \tau\theta\left(\frac{\gamma+1}{2}\right)\frac{\partial \bar{q}_{10}}{\partial \bar{x}_1}. \tag{2.12}$$

Case 2. When $|\theta| \ll \tau^{\frac{1}{2}}$,

$$\frac{1}{a^*}\frac{d\theta}{dt} = -\tau^{\frac{3}{2}}\frac{\partial \bar{q}_{10}}{\partial \bar{x}_2}\frac{\gamma+1}{2}. \tag{2.13}$$

Case 3. When $|\theta| = O(\tau^{\frac{1}{2}})$,

$$\frac{1}{a^*}\frac{d\theta}{dt} = -\tau^{\frac{3}{2}}\frac{\gamma+1}{2}\frac{\partial \bar{q}_{10}}{\partial \bar{x}_2} + \tau\frac{\gamma+1}{2}\theta\frac{\partial \bar{q}_{10}}{\partial \bar{x}_1}. \tag{2.14}$$

Equations (2.12) and (2.13) are contained in (2.14). Thus we may use (2.14).

Similarly, on considering the expansions of the right-hand sides of (2.4) and (2.5), we find that the case $|\theta| = O(\tau^{\frac{1}{2}})$ contains the other two cases and the approximate equations are

$$a^{*-1}dx_1/dt = \tfrac{1}{2}(\gamma+1)\,\bar{q}_{10}\,\tau + \tfrac{1}{2}\theta^2 \tag{2.15}$$

and

$$a^{*-1}dx_2/dt = -\theta + \tau^{\frac{3}{2}}\bar{q}_{20}. \tag{2.16}$$

However, in the case $|\theta| = O(\tau^{\frac{1}{2}})$, which we consider in what follows, the second term on the right-hand side of (2.16) can be neglected. Now we introduce the following non-dimensional variables:

$$\bar{t} = ta^*\tau/l, \quad \bar{\theta} = \theta/\tau^{\frac{1}{2}}. \tag{2.17}$$

Thus (2.14)–(2.16) give us

$$\frac{d\bar{\theta}}{d\bar{t}} = \frac{\gamma+1}{2}\left[-\frac{\partial \bar{q}_{10}}{\partial \bar{x}_2} + \bar{\theta}\frac{\partial \bar{q}_{10}}{\partial \bar{x}_1}\right], \tag{2.18}$$

$$d\bar{x}_1/d\bar{t} = \tfrac{1}{2}(\gamma+1)\,\bar{q}_{10} + \tfrac{1}{2}\bar{\theta}^2 \tag{2.19}$$

and

$$d\bar{x}_2/d\bar{t} = -\bar{\theta}. \tag{2.20}$$

Noting that $\omega = O(\delta)$, we have the following approximations for the bicharacteristic velocity components in the unsteady flow:

$$q_1 - n_1 a = a^*[\tfrac{1}{2}(\gamma+1)\,\tau\bar{q}_{10} + \tfrac{1}{2}\theta^2] + \tfrac{1}{2}(\gamma+1)\,\omega + O(\tau\epsilon), \tag{2.21}$$

$$q_2 - n_2 a = -a^*\theta + O(\tau^{\frac{1}{2}}\delta). \tag{2.22}$$

For isentropic flow, if we retain the dominant terms in the expansion for K, we get

$$K = -\frac{\gamma+1}{2}\frac{\partial \bar{q}_{10}}{\partial \bar{x}_1}\frac{a^*\tau}{l} + O(\tau^2). \tag{2.23}$$

Equation (2.1) now reduces to

$$\frac{a^*\tau}{l}\frac{\partial \omega}{\partial \bar{t}} + \left\{a^*\tau\left(\frac{\gamma+1}{2}\bar{q}_{10} + \tfrac{1}{2}\bar{\theta}^2\right) + \frac{\gamma+1}{2}\omega\right\}\frac{1}{l}\frac{\partial \omega}{\partial \bar{x}_1} - a^*\tau^{\frac{1}{2}}\bar{\theta}\frac{\tau^{\frac{1}{2}}}{l}\frac{\partial \omega}{\partial \bar{x}_2} = -\frac{a^*\tau}{l}\frac{\gamma+1}{2}\frac{\partial \bar{q}_{10}}{\partial \bar{x}_1}\omega - a_0\,\Omega\omega, \tag{2.24}$$

where we have retained only the dominant terms and used $\delta = \epsilon$. We further assume $\epsilon = \tau$ and define a non-dimensional quantity

$$\bar{\omega} = \omega/\epsilon a^* = \omega/\tau a^*, \tag{2.25}$$

so that we get

$$a_0\,\Omega = \frac{a^*\tau}{2l}\left[\bar{\theta}\frac{\partial \bar{\theta}}{\partial \bar{x}_1^1} - \frac{\partial \bar{\theta}}{\partial \bar{x}_2^1}\right] + O(\tau^2). \tag{2.26}$$

Equation (2.24) finally reduces to

$$\frac{\partial \bar{\omega}}{\partial \bar{t}} + \left\{\frac{\gamma+1}{2}(\bar{q}_{10} + \bar{\omega}) + \tfrac{1}{2}\bar{\theta}^2\right\}\frac{\partial \bar{\omega}}{\partial \bar{x}_1} - \bar{\theta}\frac{\partial \bar{\omega}}{\partial \bar{x}_2} = (\bar{K} - \bar{\Omega})\,\bar{\omega}, \tag{2.27}$$

where

$$\bar{\Omega} = \tfrac{1}{2}\{\bar{\theta}\,\partial\bar{\theta}/\partial\bar{x}_1^1 - \partial\bar{\theta}/\partial\bar{x}_2^1\} \tag{2.28}$$

and

$$\bar{K} = -\tfrac{1}{2}(\gamma+1)\,\partial\bar{q}_{10}/\partial\bar{x}_1. \tag{2.29}$$

To study the complete history of a nonlinear pulse, we have to take the numerically computed flow field past a transonic aerofoil, solve the linear ray equations (2.18)–(2.20) to determine $\bar{\theta}$ and then solve (2.24) numerically and fit a shock wave into the solution wherever necessary. This will involve a lot of computational work. In order to proceed further analytically we present a local analysis in the next section.

3. Local analysis of (2.27) in the neighbourhood of points on the sonic line

We discuss here a local analysis of (2.27) by which we can clearly show the interplay of the effects of nonlinear steepening, two-dimensional turning and wave-front curvature. Assuming that the short wave is already in a small neighbourhood of a point $(\bar{x}_1^*, \bar{x}_2^*)$ on the sonic line, we try to compute its motion before it moves away from this small neighbourhood.

At the sonic point we have $\bar{q}_{10}^* = 0$ to the first approximation and hence in the neighbourhood of this point we can write

$$\bar{q}_{10} = \left(\frac{\partial \bar{q}_{10}}{\partial \bar{x}_1}\right)^*(\bar{x}_1 - \bar{x}_1^*) + \left(\frac{\partial \bar{q}_{10}}{\partial \bar{x}_2}\right)^*(\bar{x}_2 - \bar{x}_2^*) + \ldots. \tag{3.1}$$

Hence, from the dominant terms in (2.27), we get

$$\frac{\partial\bar{\omega}}{\partial\bar{t}}+\left\{\bar{C}_\omega\,\bar{\omega}-\bar{K}^*(\bar{x}_1-\bar{x}_1^*)+\frac{\gamma+1}{2}\left(\frac{\partial\bar{q}_{10}}{\partial\bar{x}_2}\right)^*(\bar{x}_2-\bar{x}_2^*)+\tfrac{1}{2}\bar{\theta}^2\right\}\frac{\partial\bar{\omega}}{\partial\bar{x}_1}-\bar{\theta}\frac{\partial\bar{\omega}}{\partial\bar{x}_2}=(\bar{K}^*-\bar{\Omega})\,\bar{\omega}, \tag{3.2}$$

where
$$\bar{C}_\omega=\tfrac{1}{2}(\gamma+1). \tag{3.3}$$

Using
$$\left.\begin{aligned}\xi=\bar{x}_1-\bar{x}_1^*,\quad \eta=\bar{x}_2-\bar{x}_2^*,\quad \bar{\omega}=W,\quad \bar{C}_\omega=C,\\ \bar{K}^*=k,\quad \tfrac{1}{2}(\gamma+1)\,(\partial\bar{q}_{10}/\partial\bar{x}_2)^*=l,\end{aligned}\right\} \tag{3.4}$$

the equation in the simplified notation reduces to

$$\frac{\partial W}{\partial\bar{t}}+(CW-k\xi+l\eta+\tfrac{1}{2}\bar{\theta}^2)\frac{\partial W}{\partial\xi}-\bar{\theta}\frac{\partial W}{\partial\eta}=(k-\bar{\Omega})\,W. \tag{3.5}$$

If we assume the wave front to be plane and perpendicular to the streamlines, then $\bar{\theta}=0$ and $\bar{\Omega}=0$. Equation (3.5) then reduces to

$$\frac{\partial W}{\partial\bar{t}}+(CW-k\xi')\frac{\partial W}{\partial\xi'}=kW,\quad \xi'=\xi-\frac{l}{k}\eta, \tag{3.6}$$

which is the same as the approximate equation used by Prasad (1973).

Example 1

We first consider the case when initially the wave front is plane and perpendicular to the streamlines. We therefore assume the initial wave front to be

$$\xi=d,\quad \eta=s,\quad \bar{\theta}=0\quad\text{at}\quad \bar{t}=0, \tag{3.7}$$

where d is a constant giving the initial position of the wave front and s varies along the wave front.

Now the solution of the equations

$$d\bar{\theta}/d\bar{t}=-l-k\bar{\theta}, \tag{3.8}$$

$$d\xi/d\bar{t}=-k\xi+l\eta+\tfrac{1}{2}\bar{\theta}^2 \tag{3.9}$$

and
$$d\eta/d\bar{t}=-\bar{\theta} \tag{3.10}$$

with (3.7) as initial data is

$$\bar{\theta}=-\frac{l}{k}(1-e^{-k\bar{t}}), \tag{3.11}$$

$$\eta=\frac{l}{k}\left(\bar{t}+\frac{1}{k}e^{-k\bar{t}}\right)+s-\frac{l}{k^2}, \tag{3.12}$$

$$\xi=\frac{l^2}{k^2}\bar{t}+\frac{ls}{k}-\frac{1}{2}\frac{l^2}{k^3}(3+e^{-2k\bar{t}})+\left(d-\frac{ls}{k}+\frac{2l^2}{k^3}\right)e^{-k\bar{t}}. \tag{3.13}$$

To find the mean curvature of the wave front, we note that

$$\bar{\Omega}=+\tfrac{1}{2}(\bar{\theta}\,\partial\bar{\theta}/\partial\xi'-\partial\bar{\theta}/\partial\eta').$$

$\bar{\theta}$, as given by (3.11), can be regarded as a function of $(\bar{t},s)$. It can also be regarded as a function of (ξ',η') by first solving for $\bar{t}$ and s in terms of ξ' and η' from (3.12) and (3.13) with ξ and η replaced by ξ' and η'. We can now easily show that

$$\bar{\theta}\,\partial\bar{\theta}/\partial\xi'-\partial\bar{\theta}/\partial\eta'=0.$$

That is, the wave front, which was initially taken to be plane, remains plane for all time. This agrees with the assumption that the wave front is plane in Prasad's paper. However, (3.11) shows that the wave front turns, as was shown numerically by Spee (1971). We find here that as $\bar{t}$ tends to infinity $\bar{\theta}$ tends to a limiting value $-l/k$. Therefore, the unscaled angle θ which the wave front makes is $O(\tau^{\frac{1}{2}}l/k)$, showing that in reality the wave front is almost normal to the streamlines.

Thus when the initial value of $\bar{\theta}$ is zero, (3.5) now reduces to

$$\frac{\partial W}{\partial \bar{t}} + (CW - k\xi + l\eta + \tfrac{1}{2}\bar{\theta}^2)\frac{\partial W}{\partial \xi} - \bar{\theta}\frac{\partial W}{\partial \eta} = kW. \tag{3.14}$$

A parametric representation of the solution of (3.14) is

$$W = W_0(\xi_0, \eta_0)\, e^{k\bar{t}}, \tag{3.15}$$

$$\eta = \frac{l}{k}\bar{t} + \frac{l}{k^2}e^{-k\bar{t}} - \frac{l}{k^2} + \eta_0 \tag{3.16}$$

and

$$\xi = \xi_0 e^{-k\bar{t}} + \frac{W_0 C}{k}\sinh(k\bar{t}) + \frac{l}{k}\left(\eta_0 - \frac{l}{k^2}\right)(1 - e^{-k\bar{t}}) + \frac{l^2}{k^2}\bar{t} + \frac{1}{2}\frac{l^2}{k^3}(e^{-k\bar{t}} - 1) + \frac{1}{2}\frac{l^2}{k^3}(e^{-k\bar{t}} - e^{-2k\bar{t}}), \tag{3.17}$$

where the initial distribution of W in the pulse is given by $W = W_0(\xi_0, \eta_0)$ for all points $\xi = \xi_0$, $\eta = \eta_0$.

Now, as the pulse propagates, the components of the slope, namely $\partial W/\partial \xi$ (in the ξ direction) and $\partial W/\partial \eta$ (in the η direction), at any point moving with the pulse change, and we can calculate them at any time in terms of the initial slopes $\partial W_0/\partial \xi_0$ and $\partial W_0/\partial \eta_0$:

$$\frac{\partial W}{\partial \xi} = \frac{e^{k\bar{t}}\,\partial W_0/\partial \xi_0}{e^{-k\bar{t}} + C\dfrac{\partial W_0}{\partial \xi_0}\dfrac{1}{2k}(e^{k\bar{t}} - e^{-k\bar{t}})}, \tag{3.18}$$

$$\frac{\partial W}{\partial \eta} = \frac{\left(\dfrac{\partial W_0}{\partial \eta_0} + \dfrac{l}{k}\dfrac{\partial W_0}{\partial \xi_0}\right) - \dfrac{l}{k}e^{k\bar{t}}}{e^{-k\bar{t}} + C\dfrac{\partial W_0}{\partial \xi_0}\dfrac{1}{2k}(e^{k\bar{t}} - e^{-k\bar{t}})}. \tag{3.19}$$

Thus the components of the slope at a point moving with the pulse become infinite at some time if the initial component of the slope in the ξ direction is negative. Thus a shock wave first appears in the continuous pulse at a time given by

$$T = \frac{1}{2k}\log_e\left[\left\{\frac{C}{2k}\left(\frac{\partial W_0}{\partial \xi_0}\right)_{\min} - 1\right\}\Big/\frac{C}{2k}\left(\frac{\partial W_0}{\partial \xi_0}\right)_{\min}\right], \tag{3.20}$$

which is the same as the value of T obtained by Prasad (1973).

The shock motion. This may be found easily by using the result that for a weak shock the components of its velocity are the arithmetic means of the corresponding components of the bicharacteristic velocity just ahead of and just behind the shock. This can be easily deduced from the characteristic equations of the jump condition

of (3.14) across the shock front $\phi(x_\alpha, t) = 0$ (see Courant & Hilbert 1962, p. 489). Thus the shock position (ξ_s, η_s) can be obtained from

$$d\xi_s/d\bar{t} = \tfrac{1}{2}C\{W_a(\xi_s, \eta_s, \bar{t}) + W_b(\xi_s, \eta_s, \bar{t})\} - k\xi_s + l\eta_s + \tfrac{1}{2}\bar{\theta}^2, \tag{3.21}$$

$$d\eta_s/d\bar{t} = -\bar{\theta}, \tag{3.22}$$

where the suffixes a and b refer to the values of W just ahead of and just behind the shock.

Example 2

Here we consider the case in which the initial value of $\bar{\theta}$ is non-zero, say $\bar{\theta} = \theta_0$ at $\bar{t} = 0$. Therefore we assume the initial wave front to be

$$\xi = \xi_{f0}(s), \quad \eta = \eta_{f0}(s) \quad \text{at} \quad \bar{t} = 0, \tag{3.23}$$

where ξ_{f0} and η_{f0} are given by

$$\left.\begin{aligned} \xi_{f0} &= d\cos\theta_0 - s\sin\theta_0, \\ \eta_{f0} &= d\sin\theta_0 + s\cos\theta_0, \end{aligned}\right\} \tag{3.24}$$

with d a constant.

Thus solution of (3.8)–(3.10) with (3.23) as initial data gives the following values of $\bar{\theta}$, η and ξ at the wave front:

$$\bar{\theta} = \frac{l}{k}(e^{-k\bar{t}} - 1) + \theta_0 e^{-k\bar{t}}, \tag{3.25}$$

$$\eta = \eta_{f0} + \frac{l}{k}\bar{t} + (e^{-k\bar{t}} - 1)\left(\frac{\theta_0}{k} + \frac{l}{k^2}\right) \tag{3.26}$$

and

$$\begin{aligned} \xi = \frac{l^2}{k^2}\bar{t} + \frac{l\eta_{f0}}{k} - \frac{1}{2}\frac{l^2}{k^3}(3 + e^{-2k\bar{t}}) + \left(\xi_{f0} - \frac{l\eta_{f0}}{k} + \frac{2l^2}{k^3}\right)e^{-k\bar{t}} \\ - \frac{l\theta_0}{k^2} - \frac{1}{2}\frac{\theta_0^2}{k}e^{-2k\bar{t}} - \frac{l\theta_0}{k^2}e^{-2k\bar{t}} + \left(\frac{2l\theta_0}{k^2} + \frac{1}{2}\frac{\theta_0^2}{k}\right)e^{-k\bar{t}}. \end{aligned} \tag{3.27}$$

Using the same procedure as in example 1, we can easily show that

$$\begin{aligned} \bar{\Omega} = \tfrac{1}{2}[\theta_0(l + k\theta_0)e^{-k\bar{t}}\cos\theta_0 - (l + k\theta_0)e^{-k\bar{t}}\sin\theta_0] \Big/ \Big[\Big\{k\left(\xi_{f0} - \frac{l\eta_{f0}}{k}\right) \\ + \theta_0^2(\tfrac{1}{2} - e^{-k\bar{t}}) + \frac{l\theta_0}{k}(1 - e^{-k\bar{t}})\Big\}\cos\theta_0 - \Big\{\frac{l}{k}(1 - e^{-k\bar{t}}) - \theta_0 e^{-k\bar{t}}\Big\}\sin\theta_0\Big]. \end{aligned} \tag{3.28}$$

Different points on the wave front are initially characterized by different values of s. Equations (3.26) and (3.27) give the successive positions of the wave front moving along a ray starting from a point s, and the values of $\bar{\theta}$ and $\bar{\Omega}(s, \bar{t})$ along the ray are given by (3.25) and (3.28). To find the distribution of W within the pulse, we need to use the expressions for $\bar{\theta}$ and $\bar{\Omega}$ in (3.5). We note that $\bar{\theta}$ is a function of $\bar{t}$ only but that $\bar{\Omega}$ depends also on s, which makes integration of (3.5) complicated. Since we are considering a short wave, i.e. the extent of the wave in the normal direction is small compared with that along the wave front, we replace s by an approximate value $-\xi_0\sin\theta_0 + \eta_0\cos\theta_0$. From (3.24) we note that at the wave front the value of $-\xi_0\sin\theta_0 + \eta_0\cos\theta_0$ is the same as that of s. Using the value of $\bar{\theta}$ from (3.25) and

the value of $\bar{\Omega}$ from (3.28) with $s = -\xi_0 \sin\theta_0 + \eta_0 \cos\theta_0$, we can solve (3.5) with initial conditions

$$\xi = \xi_0, \quad \eta = \eta_0, \quad W = W_0(\xi_0, \eta_0) \quad \text{at} \quad \bar{t} = 0. \tag{3.29}$$

The solution is

$$\begin{aligned} W = W_0 e^{k\bar{t}} \Big[& \{ (k(d\cos\theta_0 + \xi_0 \sin^2\theta_0 - \eta_0 \sin\theta_0 \cos\theta_0) - l(d\sin\theta_0 - \xi_0 \sin\theta_0 \cos\theta_0 \\ & + \eta_0 \cos^2\theta_0) - \tfrac{1}{2}\theta_0^2) \cos\theta_0 + \theta_0 \sin\theta_0 \} \Big/ \Big\{ \Big(k(d\cos\theta_0 + \xi_0 \sin^2\theta_0 - \eta_0 \sin\theta_0 \cos\theta_0) \\ & - l(d\sin\theta_0 - \xi_0 \sin\theta_0 \cos\theta_0 + \eta_0 \cos^2\theta_0) + \theta_0^2(\tfrac{1}{2} - e^{-k\bar{t}}) \\ & + \frac{l\theta_0}{k}(1 - e^{-k\bar{t}}) \Big) \cos\theta_0 - \Big(\frac{l}{k}(1 - e^{-k\bar{t}}) - \theta_0 e^{-k\bar{t}} \Big) \sin\theta_0 \Big\} \Big]^{\frac{1}{2}}, \end{aligned} \tag{3.30}$$

and

$$\eta = \eta_0 + \frac{l}{k}\bar{t} + \left(\frac{l}{k^2} + \frac{\theta_0}{k} \right)(e^{-k\bar{t}} - 1) \tag{3.31}$$

$$\begin{aligned} \xi = {} & \frac{2CW_0}{k} e^{-k\bar{t}} \frac{A^{\frac{1}{2}}c^2}{B^{\frac{5}{2}}} \\ & \times \left[\frac{1}{4}\left(\frac{B\,e^{k\bar{t}}}{c} - 1 \right)^{\frac{1}{2}} \left(\frac{B\,e^{k\bar{t}}}{c} \right)^{\frac{3}{2}} + \frac{3}{8}\left(\frac{B\,e^{k\bar{t}}}{c} - 1 \right)^{\frac{1}{2}} \left(\frac{B\,e^{k\bar{t}}}{c} \right)^{\frac{1}{2}} + \tfrac{3}{8} \log_e \left\{ \left(\frac{B\,e^{k\bar{t}}}{c} \right)^{\frac{1}{2}} \left(\frac{B\,e^{k\bar{t}}}{c} - 1 \right)^{\frac{1}{2}} \right\} \right] \\ & + \frac{l\eta_0}{k} + \frac{l^2}{k^2}\bar{t} - \frac{3}{2}\frac{l^2}{k^3} - \frac{l\theta_0}{k^2} - \frac{1}{2}\frac{l^2}{k^3} e^{-2k\bar{t}} - \frac{1}{2}\frac{\theta_0^2}{k} e^{-2k\bar{t}} - \frac{l\theta_0}{k^2} e^{-2k\bar{t}} + \xi_0 e^{-k\bar{t}} - \frac{2cW_0}{k} e^{-k\bar{t}} \frac{A^{\frac{1}{2}}c^2}{B^{\frac{5}{2}}} \\ & \times \left[\frac{1}{4}\left(\frac{B}{c} - 1 \right)^{\frac{1}{2}} \left(\frac{B}{c} \right)^{\frac{3}{2}} + \frac{3}{8}\left(\frac{B}{c} - 1 \right)^{\frac{1}{2}} \left(\frac{B}{c} \right)^{\frac{1}{2}} + \tfrac{3}{8} \log_e \left\{ \left(\frac{B}{c} \right)^{\frac{1}{2}} + \left(\frac{B}{c} - 1 \right)^{\frac{1}{2}} \right\} \right] \\ & - \frac{l\eta_0}{k} e^{-k\bar{t}} + \frac{2l^2}{k^3} e^{-k\bar{t}} + \frac{2l\theta_0}{k^2} e^{-k\bar{t}} + \frac{1}{2}\frac{\theta_0^2}{k} e^{-k\bar{t}}, \end{aligned} \tag{3.32}$$

where

$$A = \{ k(d\cos\theta_0 + \xi_0 \sin^2\theta_0 - \eta_0 \sin\theta_0 \cos\theta_0) - l(d\sin\theta_0 - \xi_0 \sin\theta_0 \cos\theta_0 + \eta_0 \cos^2\theta_0) - \tfrac{1}{2}\theta_0^2 \} \cos\theta_0 + \theta_0 \sin\theta_0, \tag{3.32a}$$

$$B = \{ k(d\cos\theta_0 + \xi_0 \sin^2\theta_0 - \eta_0 \sin\theta_0 \cos\theta_0) - l(d\sin\theta_0 - \xi_0 \sin\theta_0 \cos\theta_0 + \eta_0 \cos^2\theta_0) + \tfrac{1}{2}\theta_0^2 + l\theta_0/k \} \cos\theta_0 - (l/k)\sin\theta_0 \tag{3.32b}$$

and

$$c = (l\theta_0/k + \theta_0^2)\cos\theta_0 + (l/k + \theta_0)\sin\theta_0. \tag{3.32c}$$

As in example 1, we can discuss the formation of a shock in the wave and follow its motion, but the expression for ξ is so complicated that it is difficult to get an expression for T, the time when a shock first appears somewhere in the pulse.

4. Numerical results and conclusion

To study the wave propagation in transonic flow we take the representative values of k and l from a calculation of the steady potential flow around a quasi-elliptical aerofoil section 0·1025–0·675–1·375 (Baurdoux & Boerstoel 1968) for which the values of the Mach number and flow inclination are given. From (2.29) and (3.4) we can calculate k and l at different points on the sonic line. The values which we have used in both examples are $k = 4{\cdot}0$ and $l = -7{\cdot}36$, which are typical values at points of the sonic line where the flow is decelerating and trapping of waves is possible (Prasad 1973). From (3.11) and (3.25) it follows that in all cases as $\bar{t}$ tends to $+\infty$, $\bar{\theta}$ tends to a limiting value $-l/k$ equal to 1·84.

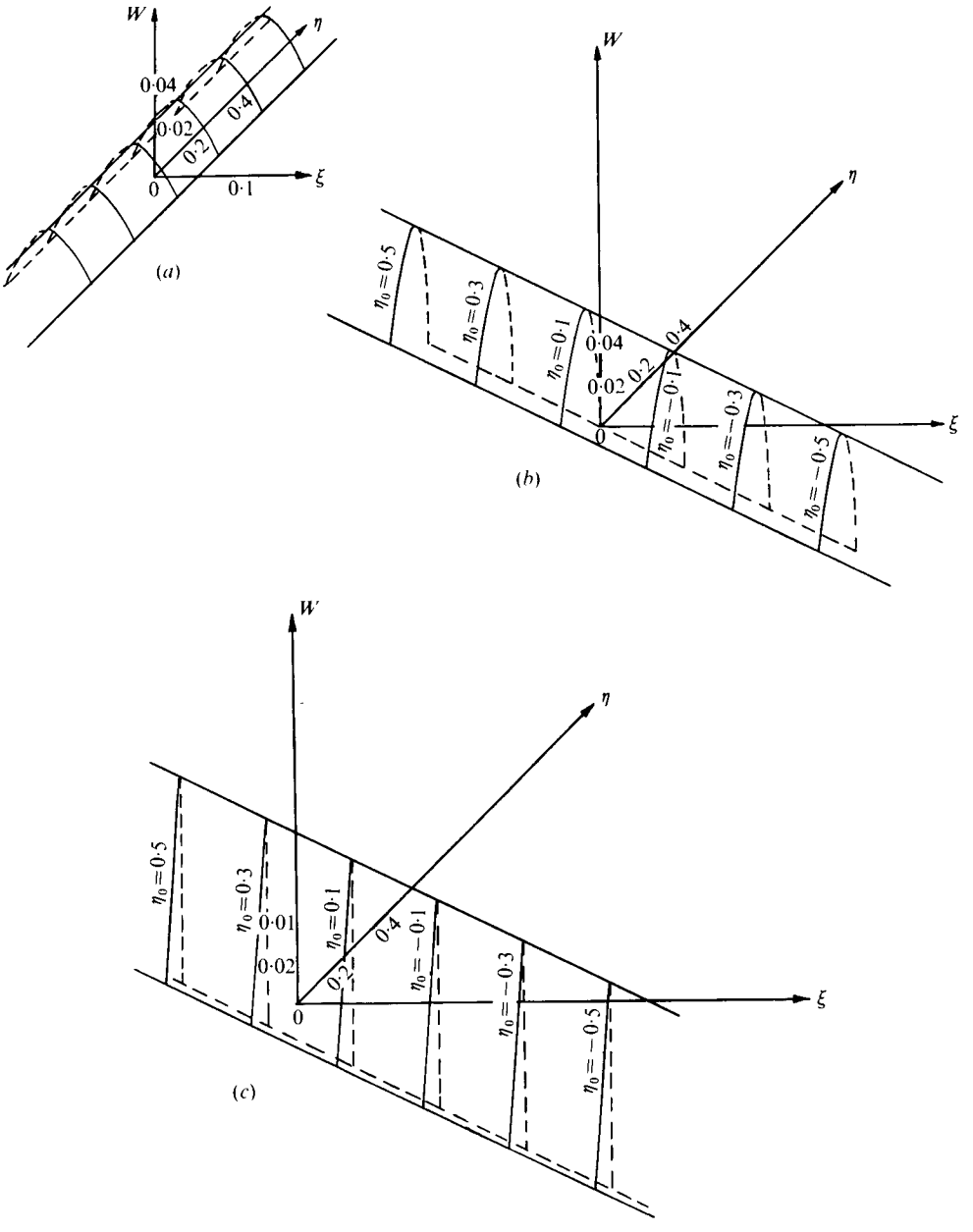

FIGURE 1. Wave profiles for $\theta_0 = 0$. (*a*) $\bar{t} = 0$, (*b*) $\bar{t} = 0{\cdot}2$, (*c*) $\bar{t} = 0{\cdot}4$.

Example 1

Here we take the initial distribution of W as

$$W = W_0(\xi_0, \eta_0) = \begin{cases} \Gamma(\beta - \xi_0)(\xi_0 - \alpha) & \text{for} \quad \alpha \leqslant \xi_0 \leqslant \beta, \\ 0 & \text{otherwise.} \end{cases}$$

For numerical computation we take α and β to be $-0{\cdot}05$ and $+0{\cdot}05$ respectively. Γ is fixed to be 10. In the derivation of the theory we assumed that $\xi = O(\delta)$ and

$\eta = O(1)$, where $\delta \ll 1$. So the range of values of ξ_0 we have taken is from $-0{\cdot}05$ to $+0{\cdot}05$ and that of η_0 is from $-0{\cdot}5$ to $+0{\cdot}5$. Equation (3.20) gives the time at which a shock appears. We find T to be equal to $0{\cdot}255$. We have drawn the pulses at $\bar{t} = 0$ (figure 1*a*), at $\bar{t} = 0{\cdot}2$ (figure 1*b*) and at $\bar{t} = 0{\cdot}4$ (figure 1*c*). In figures 1 (*b*) and (*c*), the normals to the wave fronts make angles of $1{\cdot}01\,\tau^{\frac{1}{2}}$ rad and $1{\cdot}47\,\tau^{\frac{1}{2}}$ rad respectively with the ξ direction. Since the expression for W is independent of η_0, the amplitude of the pulse at a given instant remains the same for different values of η_0. We note that, at $\bar{t} = 0{\cdot}4$, $\bar{\theta}$ has changed from 0 to $1{\cdot}47$, which is not very much different from its limiting value $1{\cdot}84$.

In drawing these figures for $\bar{t} > 0$, the scale of ξ has not been shown whereas scales of W and η have been shown. As the pulse moves, the various sections move away from each other by large distances. In the figures they are brought closer by choosing a suitable scale for ξ. When this is done the curves representing each section (which correspond to constant values of η_0) become very steep. We have used a different scale to draw the sections of the pulse. This amounts to a distortion of the pulse in the sense that the pulse should actually look much steeper than it does in the figures. In the figures we have indicated the sections by giving the values of η_0 there. At $\bar{t} = 0{\cdot}2$, figure 1 (*b*) clearly shows that the trailing front is steeper but no shock has appeared. In figure 1 (*c*), the trailing front is terminated by a shock whose amplitude has become quite large.

Example 2

In this case we have taken the initial value of $\bar{\theta}$ to be $\frac{1}{4}\pi$, i.e. the initial value of θ is $(\frac{1}{4}\pi)\,\tau^{\frac{1}{2}}$ rad. We took the same initial pulse as in example 1 but now the normal to the wave front makes a non-zero angle with the ξ axis. Therefore we chose

$$W = W_0(\xi_0, \eta_0) = \begin{cases} \Gamma\left\{\beta - \frac{1}{\sqrt{2}}(\xi_0+\eta_0)\right\}\left\{\frac{1}{\sqrt{2}}(\xi_0+\eta_0) - \alpha\right\} & \text{for} \quad \alpha < \frac{1}{\sqrt{2}}(\xi_0+\eta_0) < \beta, \\ 0 \quad \text{otherwise.} \end{cases}$$

The values of α, β and Γ are the same as in example 1. In this case we have drawn the pulses for $\bar{t} = 0$, $\bar{t} = 0{\cdot}2$, $\bar{t} = 0{\cdot}35$ and $\bar{t} = 0{\cdot}4$ (figure 2). The remark about the scales of ξ_0 and η_0 in example 1 is valid here also. At $\bar{t} = 0{\cdot}2$, $0{\cdot}35$ and $0{\cdot}4$, the normals to the wave fronts make angles of $1{\cdot}37\,\tau^{\frac{1}{2}}$, $1{\cdot}58\,\tau^{\frac{1}{2}}$ and $1{\cdot}63\,\tau^{\frac{1}{2}}$ rad respectively with the ξ axis. We note the following important points which distinguish example 2 from example 1.

(i) The amplitude of the wave now depends on s, i.e. it is different at various normal sections of the wave. Therefore, unlike example 1, the height of the pulse is not uniform.

(ii) We have not fitted the shock into the pulses (figures 2*c*, *d*). However, figure 2 (*c*) shows that W has become multi-valued at $\eta_0 = 0$, $\eta_0 = 0{\cdot}2$ and $\eta_0 = 0{\cdot}4$ but not at $\eta_0 = -0{\cdot}2$. The shock appears only in a portion of the profile and it is very difficult to follow it up. In figure 2 (*d*), the shock is present at every section.

(iii) The denominator in the expression for the curvature given by (3.28) becomes zero and then negative at $\bar{t} = 0{\cdot}2$ for certain values of s. This shows that the wave front develops a kink (which we have not shown in the figures) and changes its direction abruptly. This confirms analytically the situation shown in figure 18 in Spee's (1971) article.

The authors are grateful to Dr S. K. Chakrabartty for valuable discussions.

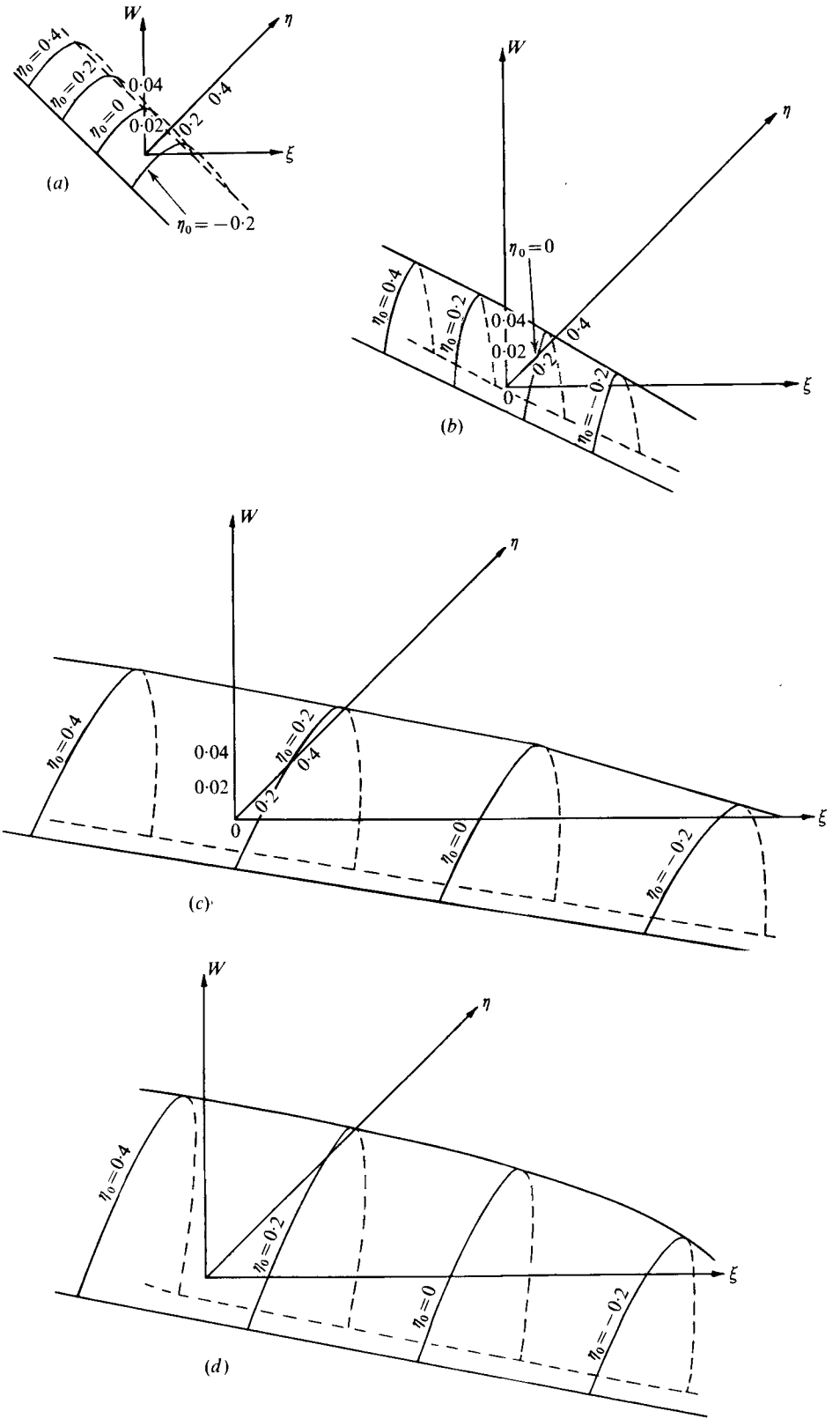

FIGURE 2. Wave profiles for $\theta_0 = \frac{1}{4}\pi$. (*a*) $\bar{t} = 0$, (*b*) $\bar{t} = 0{\cdot}2$, (*c*) $\bar{t} = 0{\cdot}35$, (*d*) $\bar{t} = 0{\cdot}4$.

REFERENCES

BAURDOUX, H. I. & BOERSTOEL, J. W. 1968 Symmetrical transonic potential flows around quasielliptical aerofoil sections. *Nat. Luch-en Ruimtevaartlab. Rep.* NLR-TR69007U.

COURANT, R. & HILBERT, D. 1962 *Methods of Mathematical Physics*, vol. 2. Interscience.

GUDERLEY, K. G. 1962 *Theory of Compressible Flow.* Pergamon.

KUO, Y. H. 1951 On the stability of two-dimensional smooth transonic flows. *J. Aero. Sci.* **18**, 1.

PRASAD, P. 1973 Nonlinear wave propagation on an arbitrary steady transonic flow. *J. Fluid Mech.* **57**, 721.

PRASAD, P. 1975 Approximation of the perturbation equations of a quasi-linear hyperbolic system in the neighbourhood of a bicharacteristic. *J. Math. Anal. Appl.* **50**, 470.

SPEE, B. M. 1971 Investigations on the transonic flow around aerofoils. *Nat. Luch-en Ruimtevaartlab. Rep.* NLR-TR69122U.